

# FINAL DESIGN OF THE FULLY EQUIPPED HWR CAVITIES FOR SARAF

G. Ferrand<sup>†</sup>, L. Boudjaoui, P. Hardy, F. Leseigneur, C. Madec, N. Misiara, N. Pichoff CEA-Saclay, DRF/IRFU/SACM-SIS, Gif-sur-Yvette, France

## Abstract

SNRC and CEA collaborate to the upgrade of the SARAF accelerator to 5 mA CW 40 MeV deuteron and proton beams (Phase 2). CEA is in charge of the design, construction and commissioning of the superconducting linac (SARAF-LINAC Project). The SCL is made up of 4 cryomodules: the first two will host each 6 half-wave resonator (HWR) low beta cavities ( $\beta = 0.09$ ) at 176 MHz; the last two will host each 7 HWR high-beta cavities ( $\beta = 0.18$ ) at 176 MHz. The fully equipped cavity includes the niobium cavity with a helium tank, an input power couplers and a frequency tuning system. The final RF design of the low and high beta cavities will be presented in this poster, as well as the RF design of the couplers, the expected tuning range of the cavities and the multipactor analysis.

## INTRODUCTION

The SARAF-LINAC project, managed by CEA (France), is integrated to the SARAF-Phase 2 project managed by SNRC (Israel) and is described in [1].

The beam dynamics studies allowed to define the accelerating voltage, 1.0 and 2.3 MV, the  $\beta_{opt}$ , 0.09 and 0.18, and the flange-to-flange length for RF cavities, 280 mm and 410 mm respectively.

Figure 1 shows the cavity with its helium tank, power coupler and the frequency tuning system.

## RF DESIGN

The frequency was defined to be 176.000 MHz in nominal operations. The optimal  $\beta$ ,  $\beta_{opt}$ , of the cavities is defined by the  $\beta$  that maximizes the R/Q ratio at 176.000 MHz. The target values are  $0.091$  and  $0.181 \pm 0.001$ . The accelerating fields are defined at  $\beta_{opt}$ . The RF design was first presented in [2]. Optimized simulation results for the low and high beta cavities are detailed in Table 1. RF power loss was computed for a niobium surface resistivity of  $40 \text{ n}\Omega$  at 4.45 K.

Table 1: Parameters of the Low and High Beta Cavities

	Low $\beta$ cav.	High $\beta$ cav.
$\beta_{opt}$	0.091	0.181
Required $E_{acc}$ (MV/m)	6.5	7.5
$Ep_{kmax}$ (MV/m)	32.1	33.2
$Bp_{kmax}$ (mT)	60.9	60.5
Diss. Power@40n $\Omega$ (W)	6.16	14.4
R/Q @ $\beta_{opt}$ ( $\Omega$ )	189	280
Stored Energy (J)	4.9	14.4

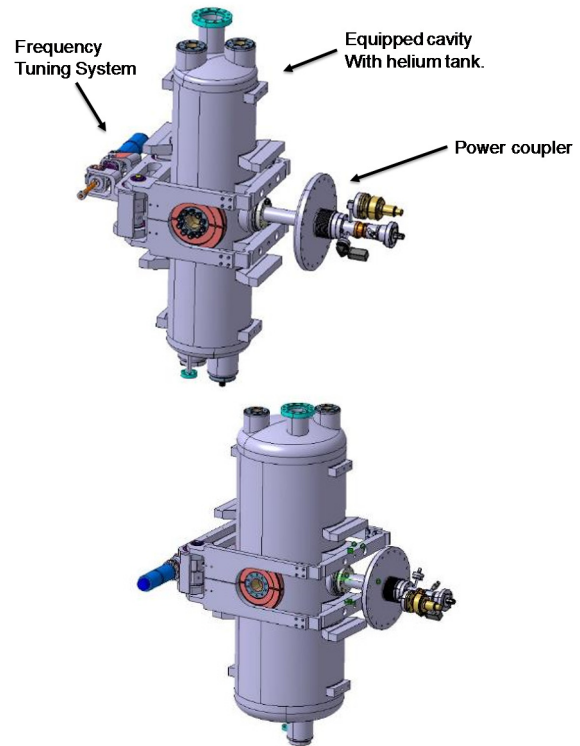


Figure 1: On the top, fully equipped low-beta cavity with power coupler and tuning system. . On the bottom, fully equipped high-beta cavity.

The field maps for the low beta cavity is presented in Figure 2. The peak electric field appears on the beam ports and drift tube. The peak magnetic field appears on the inner conductor, close to the tori.

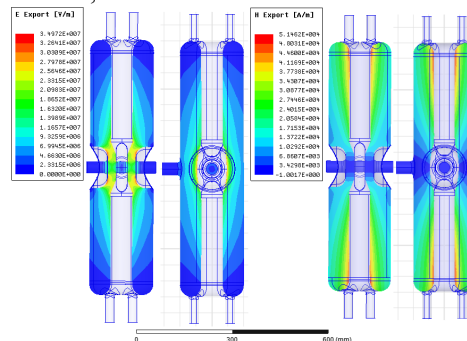


Figure 2: Electric field (left) and magnetic field (right) in the low-beta cavity.

## RF - MECHANICAL COUPLING

The cavities will be placed vertically in the cryomodules in accordance with Figure 1. The first presentation of the mechanical design can be found in [2]. Since then, new mechanical simulations were carried out in order to verify the requirements for the frequency tuner system, the sensitivity

to the helium bath pressure, and the displacement requirement on the beam port to reach the 0-100 kHz tuning range. To this purpose, we added all the other components: the string to the cold mass frame, the coupler, and the frequency tuning system. Details on the mechanical design are presented in [3].

The proposed frequency tuner system is drawn in Figure 3. It will mechanically compress the beam ports. The compression leading to the displacement of the beam flanges is induced by a step motor with a worm drive that brings lever arms closer each other. Frequency shifts were estimated with the small perturbation method. Main RF / mechanical coupling results, with the final cavity design are summed up in Table 2.

Table 2: Mechanical Properties of The Cavities (BP: Beam port)

	Low $\beta$	High $\beta$
Acceptable Pressure (bar)	2.0	2.0
Pressure Sens. (Hz/mbar)	-7.4	3.3
BP sensitivity (kHz/mm)	653	158
Required BP Displacmt (mm)	0.15	0.63
Tuning Range (kHz)	0-100	0-100

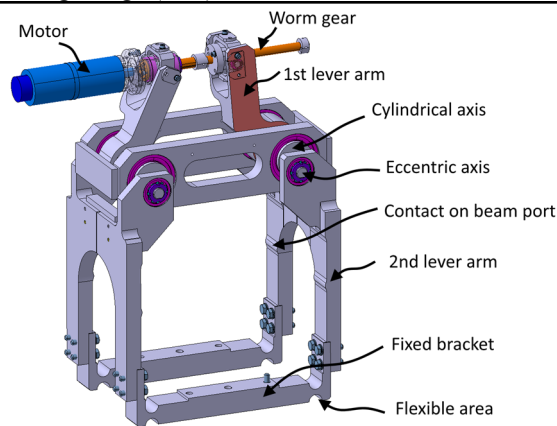


Figure 3: Drawing of the frequency tuning system (low beta cavity).

## POWER COUPLERS

The RF power requirements are 5 kW and 11 kW for low and high beta cavities. The couplers were designed for a maximal RF power of 20 kW. The external diameter of the power coupler will be 36.8 mm, to be connected to a standard EIA 1 5/8" (37.8 mm). It will be divided into two parts: a coaxial line from the cryomodule flange to the cavity flange (about 200 mm long), and a second coaxial line, outside of the cryomodule, with the warm ceramic window, diagnostics, and a thermalized forced air flow (about 100 mm long).

The antenna will be built in bulk copper, to minimize the RF power losses and optimize the thermal conductivity. The external wall of the coupler will be a single copper coated stainless steel wall, cooled by a thermal intercept at 60 K, 100 mm from the cavity flange. The coupler is de-

signed to optimize the RF matching at 176 MHz. Their external quality factors are  $Q_{ext} = 1.1 \cdot 10^6$  and  $1.7 \cdot 10^6$  for low and high beta cavities respectively.

To compensate the thermal displacement of the cavity flange with respect to the cryomodule flange, the bellow will be placed between atmosphere and cryomodule vacuum. No bellow appears on the cavity vacuum side, thus the RF connection to external coaxial line moves with the cavity. The small area where external pressure applies implies no excessive pressure load on the cavity. No barometric compensator is required. Figure 4 shows a cut of the coupler with bellow, warm window and diagnostics.

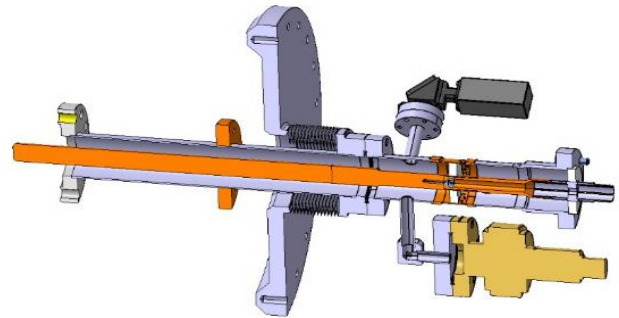


Figure 4: Cut of the coupler with diagnostics.

## PICK-UP ANTENNA

The pick-up antenna will be a loop, located in one of the HPR ports. A 3D model of the pick-up antenna is presented in Figure 5. The HPR ports have a 30-mm diameter: the dimension was defined to optimize the accessibility of the different parts of the cavity during high pressure rinsing. For both cavities, and for a target output power of 1 W, the dissipated power on the pick-up probe is only 0.8 mW ( $RRR = 20$ ). The maximum magnetic field reaches 16 A/m on the flange, i.e. 20  $\mu$ T. Even considering a flange in stainless steel (with a surface resistance of 23  $m\Omega$ ), the dissipated power on the flange should not exceed 0.2 mW for a total dissipated power close to 1 mW.

The accurate bending of the copper wire and the weld of the extremity to the flange are the challenges for this pick-up.

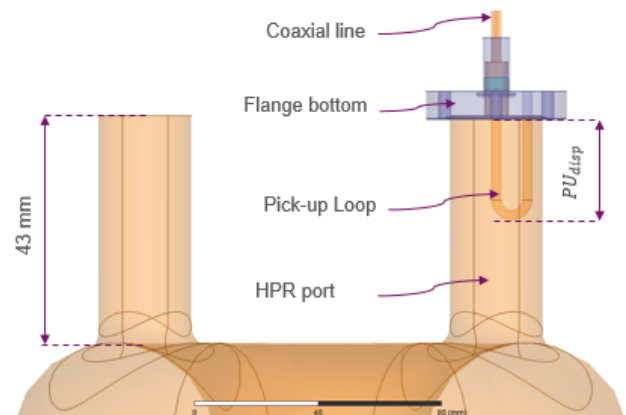


Figure 5: Drawing of the pick-up antenna in the HPR port.

## MULTIPACTOR SIMULATIONS

Multipactor simulations were carried out with Musicc3D, a software developed by the IPNO [4]. The code was validated with observations on IFMIF and Spiral 2 cavities. Simulations on SARAF cavities show very similar results to observations for IFMIF [5] and Spiral 2 [6] cavities.

Two ranges of barriers appear: one at very low accelerating field, around 50 kV/m, and one at high accelerating field, around 2 MV/m. The barriers around 50 kV/m appear in the coaxial region, and can lead to longer conditioning procedures with a  $\beta = 1$  antenna. They have no impact for operations in cryomodule with the final coupler.

The second barrier around 2 MV/m appears in the torus region. This barrier was always observed for IFMIF and Spiral 2, but it only required a few minutes to be conditioned. Experience on Spiral 2 showed no impact of this multipactor barrier on the cryogenic consumption.

Figure 6 shows the trajectory of a two points multipactor in the torus of the SARAF cavity for an accelerating field of 2.4 MV/m.

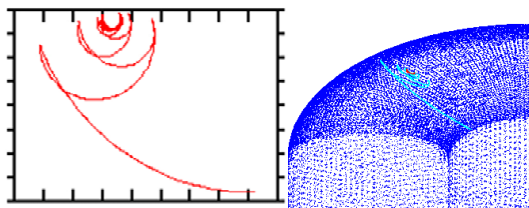


Figure 6 : Trajectory of a two points multipactor in the torus of the SARAF cavity.

## CONCLUSION

Developments on the equipped superconducting resonators are in progress at CEA for the SARAF phase II Linac. Final designs of the components were validated in June 2016. We are launching the call for tender for prototype manufacturing and expect to test the first cavity prototypes in September 2017.

## REFERENCES

- [1] N. Pichoff *et al.*, “The SARAF-Linac Project for SARAF-Phase 2”, in *Proc. 6<sup>th</sup> Int. Particle Accelerator Conf. (IPAC’15)*, Richmond, VA, USA, May 2015, paper THPF005, pp. 3683-3685.
- [2] G. Ferrand *et al.*, “Design of the HWR Cavities for SARAF”, in *Proc. 7<sup>th</sup> Int. Particle Accelerator Conf. (IPAC’16)*, Busan, South-Korea, May 2016, paper WEPMB003, pp. 2119-2121.
- [3] N. Misiara *et al.*, “Mechanical Design of the HWR Cavities for the SARAF SRF LINAC”, in *Proc. 28<sup>th</sup> Linear Accelerator Conf. (LINAC’16)*, East Lansing, MI, USA, Sep 2016, paper MOPRC026.
- [4] T. Hamelin *et al.*, “Musicc3d: A Code for Modeling the Multipacting”, in *Proc. 16<sup>th</sup> Int. Conf. on RF Superconductivity (SRF’13)*, Paris, France, Sep. 2013, paper TUP092, pp. 683-685.
- [5] N. Bazin *et al.*, “Cavity Development for the Linear IFMIF Prototype Accelerator”, in *Proc. 16<sup>th</sup> Int. Conf. on RF Superconductivity (SRF’13)*, Paris, France, Sep. 2013, paper THIOD03, pp. 878-883.

- [6] P.-E. Bernaudin *et al.*, “Tests of the Low Beta Cavities and Cryomodules for the Spiral 2 LINAC”, in *Proc. 14<sup>th</sup> Int. Conf. on RF Superconductivity (SRF’09)*, Berlin, Germany, Sep. 2009, paper TUPPO003, pp. 171-175.